Eur. Phys. J. D **30**, 393–401 (2004)
DOI: 10.1140/epjd/e2004-00107-2

THE EUROPEAN PHYSICAL JOURNAL D

Critical slowing down in a bistable model with squeezed vacuum environment

S.S. Hassan[1,a] and Y.A. Sharaby[2]

[1] University of Bahrain, College of Science, Mathematics Department, P.O. Box 32038, Bahrain
[2] Suez Canal University, Faculty of Education, Physics Department, Suez, Egypt

Received 26 December 2003 / Received in final form 25 April 2004
Published online 24 August 2004 –

Abstract. Critical slowing down effect in a bistable model of a two-level atomic medium in a ring cavity and in contact with squeezed vacuum field is examined within the mean field approximations in the high-, low- and arbitrary-Q cavity cases. Depending on the squeezed vacuum field phase parameter, the time response to linear perturbation of the incident field near the swtiching-on point can be enhanced or reduced compared with the normal vacuum case. In the low-Q cavity case with atomic collisional broadening switching time is both increased and become insensitive to the phase of the squeezed vacuum field. Analytical expressions are given and analysed for the critical (extermal) values of the incident field. In the high-Q cavity, Gaussian field feature causes lesser-steep transition between the stable states in both the normal and squeezed vacuum cases.

PACS. 42.65.Pc Optical bistability, multistability, and switching, including local field effects – 42.65.-k Nonlinear optics

1 Introduction

Theoretical study of optical bistable (OB) systems of 2-level atomic medium placed in an optical cavity where the atomic medium is in interaction with a squeezed vacuum (SV) input field has been carried out by some authors in recent years [1–6]. The use of the SV inputs in OB systems, as compared with the normal vacuum (NV) case [7–12] has characteristic features, such as:

(i) occurrence of the bistable behavior at a lower threshold value for the atomic cooperativity parameter $C = 2$ for some range of the SV field parameters [5], compared with $C = 4$ in the NV case [7];
(ii) novel "phase switching effect" [2] for the output field versus the phase of the SV field of various "isola" and "mushroom" shapes [5] depending on the detuning parameters;
(iii) linear stability analysis shows that [5] the unstable modes are not in symmetric pairs for squeeze phase values Φ such that $\sin\Phi \neq 0$.

An interesting phenomenon related to the switching aspects of the OB devices called critical slowing down (CSD). CSD is an intrinsically physical phenomenon known in phase transition theory, e.g., [13], where at the critical (switching on/off) points of the OB curve the system relaxation time diverges and so the system switches very slowly (after a time delay τ) to another stable state. Bonifacio and Meystre [14] have investigated this phenomenon, for OB model with high-Q ring cavity in the NV case, through a linear evaluation of a small perturbation of the steady state output field when the injected field approaches the critical (switching-on) point. An alternative slowing down effect was discussed by Erneux and Mandel [15] based on a non-linear evolution of the system on both sides of the critical point without adiabatic elemination scheme as in [14]. Also, effect of periodic perturbation of the input field amplitude in dispersive OB system near a critical point shows that CSD can be utilised for dynamical stabilisation [16].

In this paper, we investigate the phenomenon of CSD related to OB system in contact with SV reservior. Particularly, within the mean field limit and plane wave approximations we examine the effect of the SV field parameters on the switching-on response in the cases of absorptive and dispersive OB systems and in both the high- and low-Q cavity limits. Also the effect of the radial (transverse) field variation on the CSD in both the NV and SV cases is examined in the high-Q cavity limit.

The paper is represented as follows: the model Maxwell-Bloch equations and analysis of the field critical switching values is given in Section 2. The examination of the CSD near the switching-on point in the high-, low- and arbitrary-Q cavity cases is given in Sections 3–5 respectively. Effect of the Gaussian transverse field feature

[a] e-mail: shoukryhassan@hotmail.com

on the CSD in the high-Q cavity case is examined in Section 6 followed by a summary in Section 7.

2 Model equations and critical switching values

Consider a single mode ring cavity containing a homogeneously broadened 2-level atomic medium of length L with an input field E_I at the mirror M_1 (Fig. 1). The introduction of the SV field at mirror M_2 is credited to the authors of [4] to avoid mismatch and diffraction problems and neglect the coupling of cavity field with the SV field. The two mirrors M_1 and M_2 have reflectivity R and transmissivity $T = 1-R$, while the mirrors M_3 and M_4 have 100% reflectivity. The total length of the cavity $L_c = 2\,(L+\ell)$ and z is the position within the atomic medium. The boundary conditions for single cavity field $E(z,t)$ at $z = 0, L$ are of the form [7]

$$E(0,t) = \sqrt{T}\; E_I(t) + R\; E(L, t-\Delta t)\; e^{-i\theta T} \tag{1a}$$

$$E(L,t) = \frac{E_T\,(t)}{\sqrt{T}}. \tag{1b}$$

Here $\Delta t = (2\,\ell + L)/c$ is the time taken by the light to travel from M_2 to M_1, c is the velocity of light in vacuum, $\theta = L_c\,(\omega_c - \omega_d)/c$ is the normalized cavity detuning parameter, ω_c is the frequency of the cavity mode and ω_d is the frequency of the incident field. The decay rate of the cavity is defined by $\kappa = c/L_c$.

The reduced Maxwell equation for the cavity field $\alpha \equiv E(z,t)$ is of the form,

$$\alpha_t + c\alpha_z = g\; r_- \tag{2}$$

where g is the coupling between the cavity field and the atoms and $\alpha_t = \partial\alpha/\partial t,\ \alpha_z = \partial\alpha/\partial z$.

The Bloch equations for the atomic system driven by the cavity field α and in contact with the SV field within the rotating wave approximation and in a frame rotating at the incident field frequency ω_d are of the form [5]

$$r_{-,t} = -B\, r_- + 2g\alpha\, r_3 - \gamma\, M\, r_+ \tag{3a}$$

$$= (r_{+,t})^* \tag{3b}$$

$$r_{3,t} = -\,(B + B^*)\; r_3 - \frac{\gamma}{2} + (\alpha^*\, r_- + \text{c.c.}) \tag{3c}$$

where: $r_\pm$ are the mean values of the quadrature atomic polarization components, r_3 is the mean value of the atomic inversion, γ is the A-coefficient and $B = \gamma\,(1 + 2N + i\delta)\,/2$, $\delta = 2(\omega_o - \omega_d)/\gamma$ is the normalised atomic detuning where ω_0 is the atomic transition frequency. The squeezed vacuum parameters: N = average photon number and $M = |M|\; e^{i\,\phi_s}$ = the degree of squeezing are related for maximum squeezing by $|M|^2 = N(1+N)$ (the rigorous derivation of the Bloch equations (3) are given in Appendix A of the first reference in [5] — see also [17,18]).

According to equations (2, 3), the state equation, in the general dispersive case, which relates the normalized output and input amplitude fields $X = 2\sqrt{2}\,g\,E_T/(\gamma\sqrt{T})$, $Y = 2\sqrt{2}\,g\,E_I/(\gamma\sqrt{T})$ respectively in the steady state within the mean value limit is of the form [5],

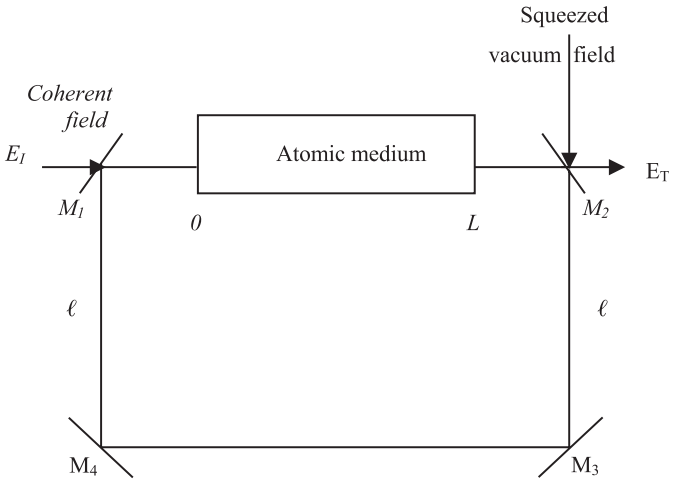

Fig. 1. The ring cavity configuration with plane mirrors.

$$Y = |X|\left|1 + i\theta + \frac{2C\,(b_1 - ib_2)}{\delta^2 - 4\,|M|^2 + (1+2N)^2 + b_1\,|X|^2}\right| \tag{4}$$

where;

$$b_1 = 1 - \frac{2\,|M|\cos\Phi}{1+2N},\ \ b_2 = \frac{\delta + 2\,|M|\sin\Phi}{1+2N}$$

and $\Phi = \phi_s - 2\phi_f$ is the relative phase of the squeezed vacuum field with respect to the output field, $X = |X|e^{i\phi_f}$, and $C = g^2/(\gamma\,\kappa)$ is the cooperative parameter.

In the absorptive case ($\delta = \theta = 0$) the effect of changing the SV field phase Φ on the switching-on value in the bistable curve of the input-output field relation is shown in Figure 2. Also, in the SV case and for phase value $\Phi = 0$, a small change in the atomic detuning from $\delta = 0$ to $\delta = 1$ results in clear shift of the switching points of the OB curve (Fig. 3) unlike the NV case [12] where the switching points is little affected within this interval of change of δ. The effect of changing the cavity detuning θ from 0 to 1 has no significant effect on the switching points for $\delta = 0$ or $\delta \neq 0$ in the SV case, henceforth we investigate the CSD near the switching-on points in the two cases: the absorptive case ($\delta = \theta = 0$) and the dispersive case ($\theta = 0$, $\delta \neq 0$).

According to the state equation (4) the critical value of the incident field (at the switching-on point) for $C \gg 1$, $\theta = 0$ and $\delta \neq 0$ is given by

$$Y_{C:SV} = \sqrt{\frac{(1 + \delta^2 + C\,b_1)^2 + C^2\,b_2^2}{b_1(1+\delta^2)}} \tag{5}$$

which is dependent on the SV parameters (N, Φ) and reduces to $Y_{C;\,NV} = C + 1$ in the NV case [14]. At resonance ($\delta = 0$), the variation of $Y_{C;\,SV}$ against Φ

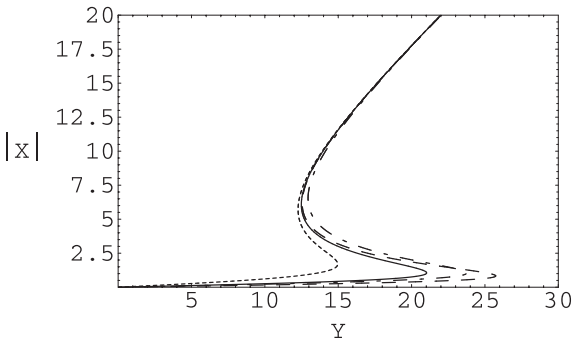

Fig. 2. The steady state output-input field amplitude curve ($|X|$ versus Y) in the absorptive case ($\theta = 0, \delta = 0$) for $C = 20$ in the NV case ($N = 0$, full line) and in SV case ($N = 0.1$) with different SV phase values $\Phi = 0$ ($\cdots$), $\pi/2$ ($-\cdot-\cdot$), π ($---$).

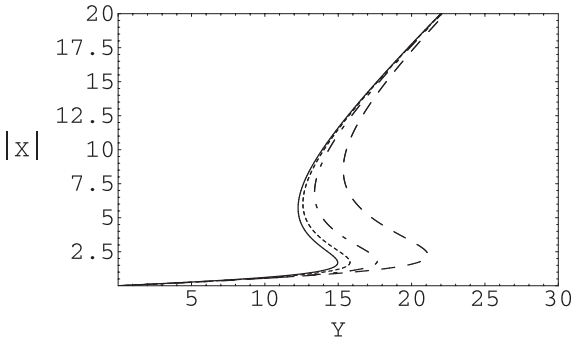

Fig. 3. The steady state output-input field amplitude curve for $C = 20$, $\theta = 0$ in the SV case ($\Phi = 0$, $N = 0.1$) and different atomic detuning values $\delta = 0$ (—), 0.25 ($\cdots$), 0.5 ($-\cdot-\cdot$) and 1 ($---$).

(for fixed values of N) and against N (for fixed values of Φ) are shown in Figures 4a and 4b. If we define $\Phi_c = \cos^{-1}[2|M|/(1+2N)]$ as the value of the SV field phase at which $Y_{C;\,SV} = Y_{C;\,NV}$ we notice that, for fixed N,

$$Y_{C;\,SV} < Y_{C;\,NV}, \quad \text{for} \quad 0 \le \Phi < \Phi_c, \tag{6a}$$

$$Y_{C;\,SV} > Y_{C;\,NV}, \quad \text{for} \quad \Phi_c \le \Phi < \pi. \tag{6b}$$

For the special values of $\Phi = 0,\ \pi/2,\ \pi$ and for $N \gg 1$ we have

$$Y_{C;\,SV} = \begin{cases} \dfrac{(C+2N)}{\sqrt{2N}}; & \Phi = 0 \\ \sqrt{(1+C)^2 + C^2}; & \Phi = \dfrac{\pi}{2} \\ \sqrt{2}\,C + \dfrac{1}{\sqrt{2}}; & \Phi = \pi \end{cases} \tag{7}$$

which implies the following inequalities for $C > 1$:

$$Y_{C;\,SV}(\Phi = 0) < Y_{C;\,NV} < Y_{C;\,SV}(\Phi = \pi/2) = Y_{C;\,SV}(\Phi = \pi) \tag{8}$$

and the smallest critical value in the SV case is $Y_{C;\,SV}$ for $\Phi = 0$. On the other hand for small N, specifically for

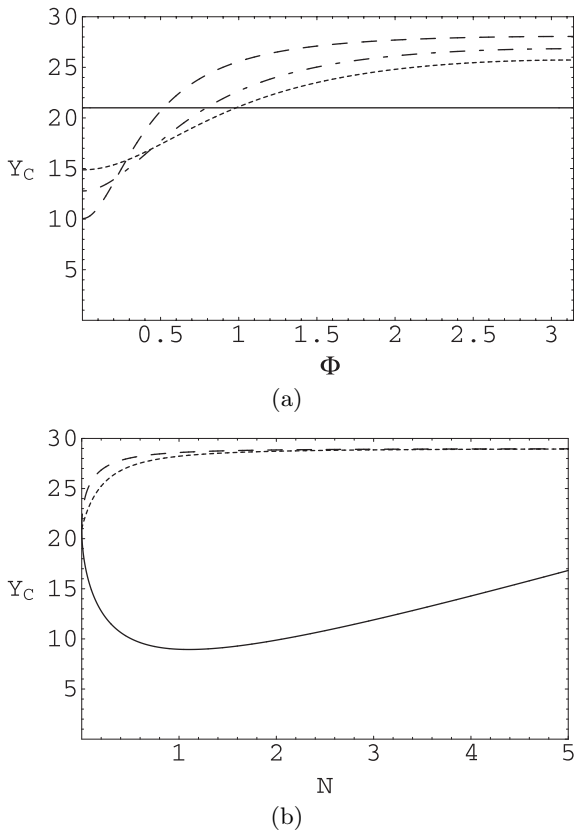

Fig. 4. (a) The variation of the critical value Y_C against the SV phase Φ for $C = 20$, $\theta = 0$, $\delta = 0$ and different values of the average photon number of the SV $N = 0.1$ ($\cdots$), 0.2 ($-\cdot-\cdot$) and 0.5 ($---$). The full line represents the NV case ($N = 0$) which is independent of Φ. (b) Y_C against N for $C = 20$, $\theta = 0$, $\delta = 0$ in the SV case with different phase values, $\Phi = 0$ (—), $\pi/2$ ($\cdots$) and π ($---$).

$4N < 1$ we have,

$$Y_{C;\,SV} = \begin{cases} \dfrac{1 + \left(1 \mp 2\sqrt{N}\right) C}{\sqrt{1 \mp 2\sqrt{N}}}; & \Phi = 0,\ \pi \\ \sqrt{(1+C)^2 + 4N\,C^2}; & \Phi = \pi/2 \end{cases} \tag{9}$$

which implies the following inequalities for $C > 1$:

$$Y_{C;\,SV}(\Phi = 0) < Y_{C;\,NV} < Y_{C;\,SV}(\Phi = \pi/2) < Y_{C;\,SV}(\Phi = \pi) \tag{10}$$

and the critical value $Y_{C;\,SV}$ for $\Phi = \pi$ is the largest compared with other cases including the NV case. The inequalities (8) and (10) are in agreement with the numerical plot in Figure 4b.

For $\delta \neq 0$ the variation of $Y_{C;\,SV}$ against Φ for different values of N is shown in Figure 5a for $C = 20$ and $\delta = 0.5$. In comparison with the absorptive case ($\delta = 0$, Fig. 4a) it increases initially at $\Phi = 0$ for some range of Φ and then decreases slowly near $\Phi = \pi/2$. This is in confirmity with

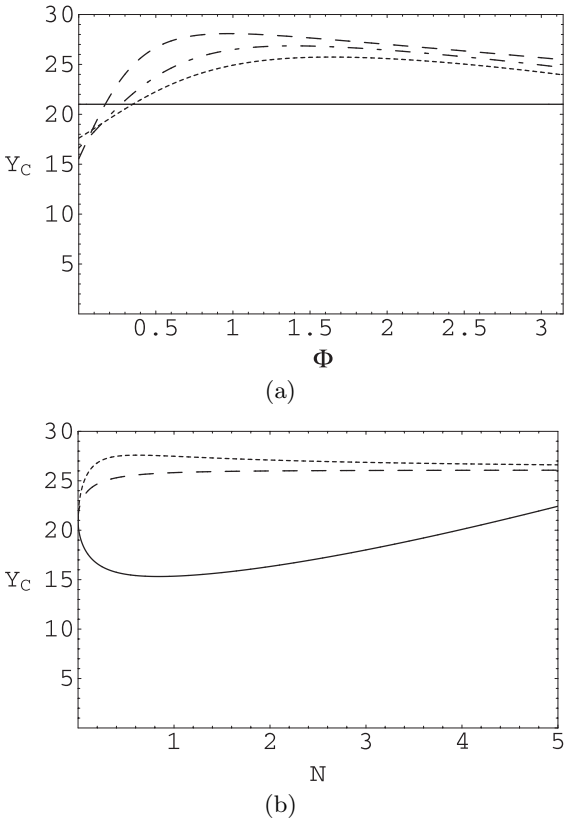

Fig. 5. (a and b) As Figures 4a and 4b respectively but with $\delta = 0.5$.

Figure 5b where $Y_{C;\,SV}(\Phi = \pi) < Y_{C;\,SV}(\Phi = \pi/2)$ as N varies, unlike the absorptive case of Figure 4b.

3 The high-Q cavity case

In this case the cavity decay rate κ is much less than the atomic decay rate $\kappa \ll \gamma$. By adiabatically eliminating the atomic variables from equations (3) we get within the mean field limit (cf. [5,7]) the time-dependent equation for the normalised output field $X(\tau)$ for $\theta = 0$ where $\tau = \kappa\, t$, in the form

$$\frac{dX(\tau)}{d\tau} = Y - X(\tau) - \frac{2C(b_1 - ib_2)X(\tau)}{1 + \delta^2 + b_1\,|X(\tau)|^2}. \qquad (11)$$

In the vicinity of $Y_{C;\,SV}$, given by equation (5) we replace $Y = Y_{C;\,SV} + \beta$, with $\beta < 1$ is a small perturbation, the numerical solutions of (11) for $C = 20$ are presented in Figures 6–8 where we notice the following:

(i) in the absorptive case ($\delta = \theta = 0$), the larger time delay to switch to the upper branch of the OB curve as Y gets closer ($\beta = 0.027$) to $Y_{C;\,NV}$ in the NV case [14] (Fig. 6a) is considerably reduced in the SV case of phase value $\Phi = \pi$ by a factor ≈5 (Fig. 6b). Qualitative behavior is also obtained for $\Phi = \pi/2$, but for $\Phi = 0$ in the absorptive case ($\delta = 0$) or dispersive case ($\theta = 0,\ \delta = 0.5$) the time delay diverges further than in the NV case. For fixed values of $\beta = 0.027$ and for $\Phi = \pi$ (similarly for $\Phi = \pi/2$) increasing N (the average photon number in the SV field) reduces also the time delay considerably (Fig. 7). The same is obtained in the dispersive case for $\theta = 0$, $\delta = 0.5$;

(ii) in the dispersive case ($\theta = 0$, $\delta = 0.5$) and in the NV case we have similar results as Figure 6a but the time delay for $\beta = 0.028,\ 0.03$ is slightly reduced. In the SV case for $\Phi = \pi$ and fixed β the increase in δ increases the time delay (Fig. 8) but for $\Phi = \pi/2$, the increase in δ slightly reduces the time delay;

(iii) the transition from the lower to the upper branch of the OB curve is in the SV case is more steeper than in the NV case.

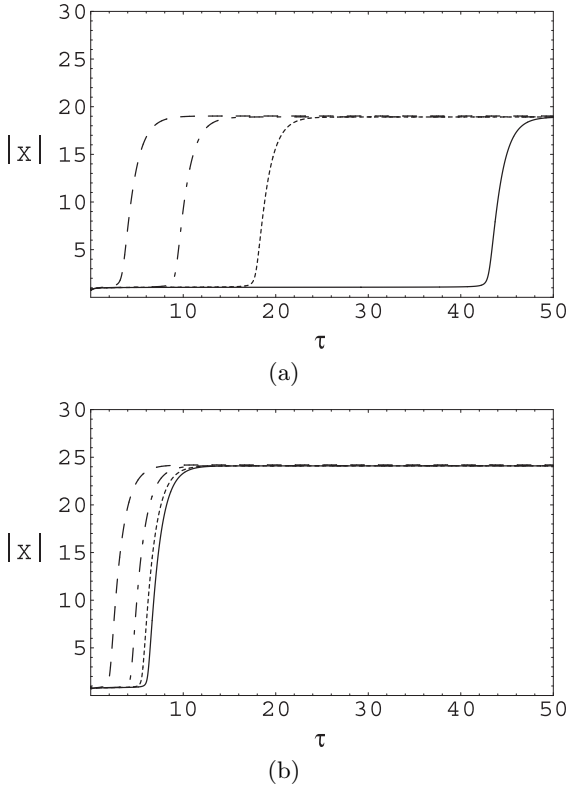

Fig. 6. (a) The transient output field $|X(\tau)|$ versus time $\tau = \kappa\, t$ in the high-Q limit for $C = 20$, ($Y_C \approx 21$), $\theta = 0$, $\delta = 0$ in the NV case ($N = 0$) and different values of the input field $Y = Y_C + \beta$; $\beta = 0.027$ (—), 0.03 ($\cdots$), 0.04 ($-\cdot-$) and 0.12 ($---$). (b) As (a) but in the SV case ($N = 0.1$, $\Phi = \pi$).

4 The low-Q cavity case

In this case the cavity decay rate is much greater than the A-coefficient, $\kappa \gg \gamma$ and the cavity field is eliminated adiabatically. Further, we consider two sub-cases.

4.1 Collision broadening

In this case the system dynamics is *only* dominated by the atomic inversion dynamics. The adiabatic elimination

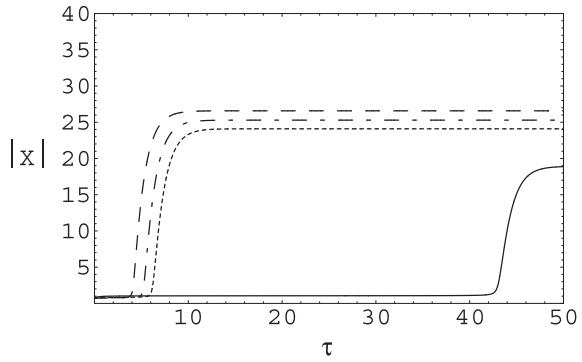

Fig. 7. The transient output field $|X(\tau)|$ versus time $\tau = \kappa\, t$ in the high-Q limit for $C = 20$, $\theta = 0$, $\delta = 0$ and fixed value of $Y = Y_C + \beta$; $\beta = 0.027$ in the SV case of $\Phi = \pi$ and various values of $N = 0.1$ $(\cdots\cdots)$, 0.2 $(-\cdot-\cdot)$ and 0.5 $(---)$. The full line represents the NV case ($N = 0$).

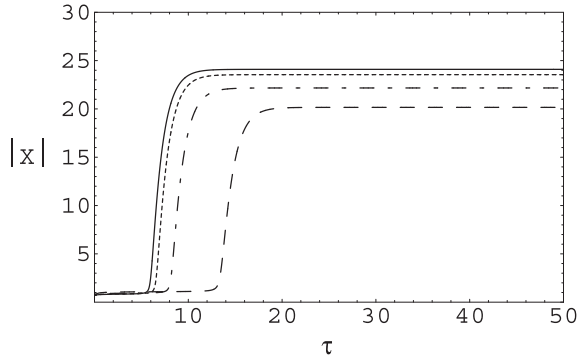

Fig. 8. As Figure 7 in the SV case ($N = 0.1$, $\Phi = \pi$) but for $\beta = 0.028$ and different values of the atomic detuning $\delta = 0$ (—), 0.25 $(\cdots\cdots)$, 0.5 $(-\cdot-\cdot)$ and 0.8 $(---)$.

of the atomic polarization is *justified* in the case where atoms collide with each other / or with the cavity walls. This leads to (transverse) decay rate for the polarization components $\gamma_\perp = \gamma(1 + 2N)/2 + \eta$ where η is a phase decay rate due to the random dephasing collision [9]. In this case equations (3a, 3b) for the atomic polarization components $r_\mp$ are of the same form but with $B \to B + \eta$, i.e.,

$$r_{-,t} = -(B\ + \eta)\, r_- + 2\, g\alpha\, r_3 - \gamma\, M\, r_+ \qquad (12a)$$

$$= (r_{+,t})^*. \qquad (12b)$$

Consequently, the steady state equation (4) is now modified for $\eta \neq 0$ to the form

$$Y = |X| \left| 1 + \frac{2\, C\, (b_1 + \frac{2\eta}{(1+2N)})}{\zeta} \; - \; i\, \frac{2\, C\, b_2}{\zeta} \right| \qquad (13)$$

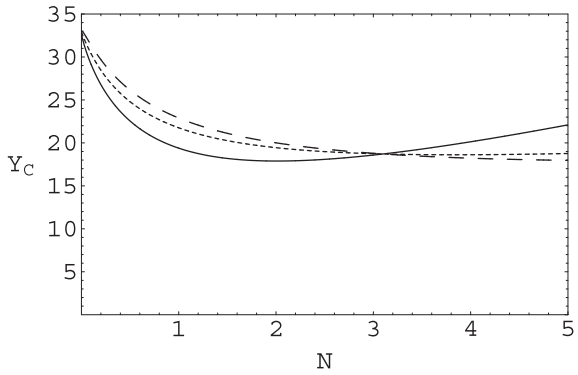

Fig. 9. The variation of the critical value Y_C in the low-Q cavity case with collisional broadening, equation (14), against the SV parameter N for $\theta = 0$, $\delta = 0$, $C = 80$, $\eta = 3$ and different values of the SV phase $\Phi = 0$ (—), $\pi/2$ $(\cdots\cdots)$ and π $(---)$.

where;

$$\zeta = 1 + \delta^2 + 4\eta^2 + 4\eta\,(1 + 2N) + |X|^2\,(b_1 + 2\eta/(1 + 2N))\,.$$

In general, the effect of the dephasing collisional parameter η on the bistable behavior of the system in both the NV and SV cases is to decrease the switch-on values of Y and hence reduces the area of the bistable device. According to equation (13), the critical value of the incident field at the switching-on point for $C \gg 1$ is given by

$$Y_{C:SV} = \sqrt{\frac{\left(1+\delta^2+4\eta^2+4\,\eta(1+2N)+C\left(b_1+\frac{2\eta}{(1+2N)}\right)\right)^2+C^2\,b_2^2}{(1+\delta^2+4\eta^2+4\,\eta\,(1+2N))\,\left(b_1+\frac{2\eta}{(1+2N)}\right)}}. \qquad (14)$$

The formula (14) varies slowly with the SV phase Φ. Indeed for $C \gg 1$, $\eta > 1$, $0 \leq N \leq 1$, $Y_{C;\,SV} = C/\sqrt{2\,\eta(1 + 2N)}$ is independent of Φ contrary to the radiative case $\gamma_{11} = 2\,\gamma_\perp$ of Figure 4a. For fixed values of Φ the variation of $Y_{C;\,SV}$ of equation (14) with N shows it decreases, except for $\Phi = 0$ it gradually increases for $N > 2$ (Fig. 9).

Now for $\eta \gg \gamma\, N$, $\gamma_\perp \gg \gamma_{11}\,(\equiv \gamma(1 + 2N))$ both $\gamma_\perp^{-1}$ and κ^{-1} are the shortest characteristic times with respect to the longitudinal decay time γ_{11}^{-1}. Thus from equations (2, 3c, 12) we get the time-dependent output field ($\tau' = \gamma\, t$),

see equation (15a) below

$$X\,(\tau') = \frac{Y}{\left[\left(1 - \frac{4\,C\,(1+2N)\;r_3\,(\tau')}{1+\delta^2+4\eta^2+4\eta\,(1+2N)}\left(b_1 + \frac{2\,\eta}{(1+2N)}\right)\right) + i\,\left(\frac{4\,C\,(1+2N)\;r_3\,(\tau')}{1+\delta^2+4\eta^2+4\eta\,(1+2N)}\,b_2\right)\right]} \qquad (15a)$$

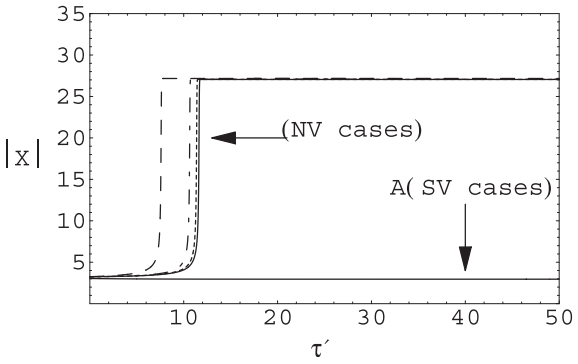

Fig. 10. The transient output field $|X(\tau')|$ versus time $\tau' = \gamma\, t$ in the low-Q cavity case with collisional broadening ($\eta = 3$) in the NV case for $C = 80$, $\theta = 0$, $\delta = 0$ and different values of the input field $Y = Y_C + \beta$; $\beta = 0.027$ (—), 0.03 ($\cdots\cdots$), 0.04 ($-\cdot-\cdot$) and 0.12 ($- - -$). Curve A represents the SV case ($N = 0.1$, $\Phi = \pi$) for the same values of β.

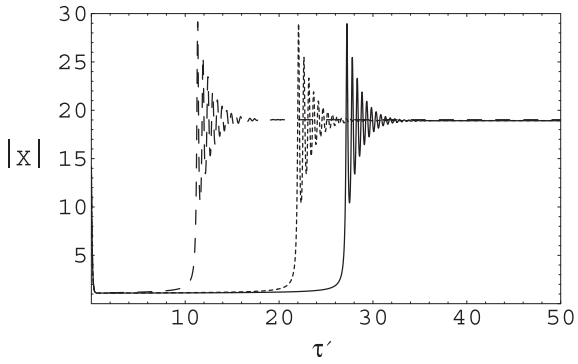

Fig. 11. (a) As Figure 10 in the low-Q cavity case with no collisional broadening ($\eta = 0$) in the NV case for $C = 20$, $\theta = 0$, $\delta = 0$ and different values of the input field $Y = Y_C + \beta$; $\beta = 0.03$ (—), 0.04 ($\cdots\cdots$) and 0.12 ($- - -$). (b) As (a) but in the SV case ($N = 0.1$, $\Phi = \pi$) — the same result is obtained for various β in (a).

where the atomic inversion $r_3(\tau')$ obeys the differential equation,

$$r_{3,\tau'} = -\frac{1}{2} - (1+2N)\; r_3\,(\tau') - \frac{(1+2N)\;|X\,(\tau')|^2\; r_3\,(\tau')}{(1+\delta^2+4\eta^2+4\eta\;(1+2N))}\left(b_1 + \frac{2\,\eta}{(1+2N)}\right). \tag{15b}$$

Equation (15b) is numerically solved after substituting for $X(\tau')$ from (15a) for $r_3(\tau')$ with initial condition, $r_3(0) = -0.2$, in the domain closed to $Y_{C;\,SV}$ and in turn $X(\tau')$ is evaluated from (15a). In the NV case for $\delta = 0$, $\eta = 3$ (Fig. 10) the time delay slightly affected as Y gets closer to $Y_{C;\,NV}$, unlike the high-Q cavity case of Figure 6a. In the SV case ($N = 0.1$, so $\eta/\gamma \gg N$) the switching time increases as $Y \to Y_{C;\,SV}$ (curve A in Fig. 10) and becomes independent of the phase value Φ. This can be explained as follows: (a) the random dephasing collision between atoms (which produces heat) decorrelates some of the SV "photon twins" and hence the switching time is weakly-dependent on the SV phase value; (b) the increase in the switching time is due to the reduction of (atomic) fluctuation caused by the SV field. This is in confirmity with the investigation of Savage and Walls [19] who showed that the tunneling time in the SV case from one state to another associated with the bistable potential well is increased compared with the NV case. Increasing the value of the collisional broadening parameter η *or* the value of the atomic detuning δ leads to a divergence delay time in both NV and SV cases.

4.2 Radiative broadening

In this case the collision broadening is absent ($\eta = 0$) and $\gamma_{11} = 2\gamma_\perp = \gamma(1+2N)$ and the system dynamics is governed by both the atomic polarization and inversion dynamics. Adiabatically eliminating the field from equation (2), substituate the result into equations (3) and defining $X = u + iv$ and $r_-(\tau') = P(\tau') + iQ(\tau')$, $\tau' = \gamma\, t$ we get the following equations

$$P_{\tau'} = \frac{1}{2}(Q(\tau')\delta - P(\tau')(1+2N)) + \frac{|M|}{|X|^2}(P(\tau')\Gamma_1 - Q(\tau')\Gamma_2) + \frac{r_3(\tau')u}{\sqrt{2}} \tag{16a}$$

$$Q_{\tau'} = -\frac{1}{2}(P(\tau')\delta + Q(\tau')(1+2N)) - \frac{|M|}{|X|^2}(P(\tau')\Gamma_2 + Q(\tau')\Gamma_1) + \frac{r_3(\tau')v}{\sqrt{2}} \tag{16b}$$

$$r_{3,\tau'} = -(1+2N)r_3(\tau') - \frac{1}{2} - \frac{1}{\sqrt{2}}(uP(\tau') + Q(\tau')v) \tag{16c}$$

where, $u = Y + 2\sqrt{2}\,C\;P$, $v = 2\sqrt{2}\,C\;Q$, $\Gamma_1 = 2uv\sin\Phi - (u^2 - v^2)\cos\Phi$ and $\Gamma_2 = 2uv\cos\Phi + (u^2 - v^2)\sin\Phi$.

Equations (14) are numerically solved with initial conditions $r_3(0) = -0.2$, $r_-(0) = -(0.282 + i\,0.234)$ for the atomic variables in the domain close to the critical value of the incident coherent field. We notice here, with the field variable only eliminated, for certain values of the system parameters the OB device remains in its lower branch for a certain time and then jumps to the upper branch with damped Rabi oscillations. For $\delta = 0$ in the NV case (Fig. 11a) the more closer $Y \to Y_{C;\,NV}$ is the larger time delay but the presence of the SV field (with suitable phase value) leads to rapid switching to the upper branch as shown in Figure 11b. For $\delta \neq 0$ up to $\delta = 0.8$, the above results are not much affected but the amplitude of oscillations are reduced as δ increased.

5 Arbitrary-Q cavity with collisional broadening

In this case we assume that the relaxation time $\gamma_\perp^{-1}$ for the polarization components $r_\pm$ is the shortest of all other

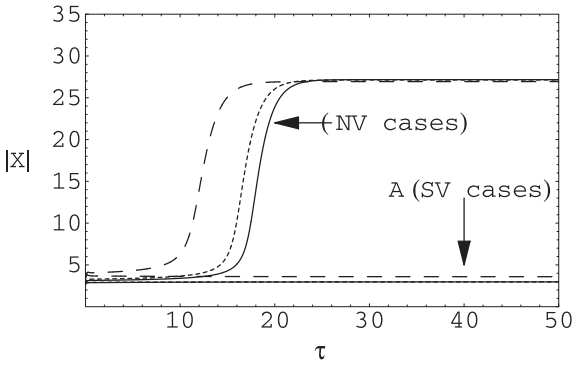

Fig. 12. The transient output field $|X(\tau)|$ versus time $\tau = \kappa\, t$ in the NV case for $C = 80$, $\beta = 0.12$, $\theta = 0, \bar{\kappa} = 1$, $\eta = 3$ and for various values of δ; $\delta = 0$ (—), 2 ($\cdot\cdot\cdot\cdot$) and 5 ($-\,-\,-$). Curves A represents the SV case ($N = 0.1$, $\Phi = \pi$).

characteristic times ($\gamma_\perp \gg \gamma_{11}$, κ) so that the atomic polarization components with phase decay $\eta \neq 0$ as governed by equation (12) are eliminated adiabatically and the system dynamics is dominated by *both* the field and atomic inversion dynamics of equations (2) and (3c) — so $\kappa \sim \gamma_{11}$. Hence we get ($\tau = \kappa\, t$, $\bar{\kappa} = \kappa/\gamma$)

$$u_\tau = Y - u + \frac{4\,C\,r_3\;(1+2N)\;\left(\left(b_1+\frac{2\eta}{1+2N}\right)\;u+v\,b_2\right)}{1+\delta^2+4\,\eta^2+4\,\eta\;(1+2N)} \tag{17a}$$

$$v_\tau = -v + \frac{4\,C\,r_3\;(1+2N)\;\left(\left(b_1+\frac{2\eta}{1+2N}\right)\;v-u\,b_2\right)}{1+\delta^2+4\,\eta^2+4\,\eta\;(1+2N)} \tag{17b}$$

$$\bar{\kappa}\,r_{3,\tau} = -\frac{1}{2} - (1+2N)\;r_3 - \frac{r_3\;(1+2N)\;|x|^2\;\left(b_1+\frac{2\eta}{1+2N}\right)}{1+\delta^2+4\,\eta^2+4\,\eta\;(1+2N)}. \tag{17c}$$

The numerical solution of equations (17) for $X(\tau)$ for $C = 80$, $\delta = 0$, $\theta = 0$ and $\eta \succ 3$ shows that the delay time diverges in both NV and SV cases. However, for fixed $\beta = 0.12$ and $\bar{\kappa} = 1$ the delay time in the NV case reduces with increased atomic detuning (it slightly increases for $\bar{\kappa} \sim 1.5$) — Figure 12. In the SV case the delay time diverges with increased δ (curves A in Fig. 12) — unlike the high-Q cavity case of Figure 8.

6 Transverse effect in the high-Q cavity case

Now taking into account the possible variations of the field along the transverse directions we can study the effect of transverse field on the CSD phenomenon in the presence of the SV field. Studies of transverse field effect on OB has been carried out in both ring and Fabry-Perot cavities [20–28] in the NV case. The effect of transverse field feature on OB in ring cavity in the presence of squeezed vacuum field for homogeneously and inhomogeneously broadened two-level atomic medium was recently examined [6]. Here we examine the effect of the transverse field profile on the time delay associated with the CSD phenomenon.

The reduced Maxwell equation, within the one transverse mode approximation for the unidirectional normalised field component $X(t)$ in the ring cavity configuration (of now spherical mirrors M_i; $i = 1{-}4$) [6,25] together with the Bloch equations for homogeneously broadened 2-level atomic system driven by a Gaussian field $\sqrt{a(\rho)}\,X(t)$ and in contact with the SV field within the mean field approximation, replace equations (2, 3) by the following form,

$$\frac{dX}{dt} = \kappa\left[Y - (1+i\theta)X + 2\sqrt{2}C\int_h^1 a(\rho)^{-\frac{1}{2}} r_-\; da(\rho)\right] \tag{18a}$$

$$r_{-,t} = -\frac{\gamma}{2}(1+2N+i\delta)\,r_- + \frac{\gamma}{\sqrt{2}}\sqrt{a(\rho)}\,X\,r_3 - M r_+ = (r_{+,t})^* \tag{18b}$$

$$r_{3,t} = -\gamma(1+2N)\,r_3 - \frac{\gamma}{2} - \frac{\gamma}{2\sqrt{2}}\sqrt{a(\rho)}(X\,r_+ + X^*\,r_-). \tag{18c}$$

Here $a(\rho) = e^{-(\frac{2\rho^2}{w_o^2})}$ is the Gaussian field shape for Fresnel number $F \gg 1$, $h = a(\rho_o) = e^{\frac{-2\rho_o^2}{w_o^2}}$ in which ρ_o is the radius of the atomic sample and w_o is the spot size or beam waist. In the high-Q cavity limit, equations (18) gives the following time-dependent equation for the output field ($\tau = \kappa\, t$),

$$\frac{dX}{d\tau} = Y - (1+i\theta)X - 2C(b_1 - ib_2)X\int_h^1 \frac{da(\rho)}{1+\delta^2+a(\rho)b_1\,|X|^2}. \tag{19}$$

The steady state input-output relation according to (19) is given by [6],

$$Y = X\left[\left(1+\frac{2C}{|X|^2}\ln A\right) + i\left(\theta - \frac{2\,C\,b_2}{b_1\,|X|^2}\ln A\right)\right] \tag{20}$$

where

$$A = \frac{1+\delta^2+b_1\,|X|^2}{1+\delta^2+b_1 h\,|X|^2}.$$

In either the absorptive or dispersive case the increase in the transverse parameter (ρ_o/w_o) in the SV case [6] on the OB curve is to increase the switching-on values (Fig. 13) as in the NV case [25] but with enlarged bistable area.

The role of the transverse parameter (ρ_o/w_o) on the delay time is shown in Figure 14 for $\delta = 0$, $\beta = 0.027$ and $C = 20$. In the NV case (Fig. 14a) the increase of (ρ_o/w_o) produces an increase in the time delay of the bistable device. While in the SV case (Fig. 14b) this time delay is

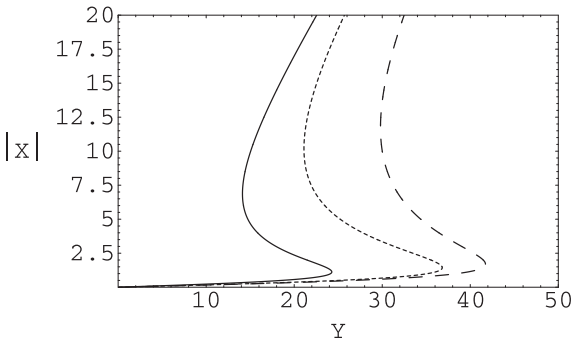

Fig. 13. The steady state output-input field amplitude curve ($|X|$ versus Y) in the SV case ($\Phi = \pi$, $N = 0.1$) for $C = 20$, $\delta = \theta = 0$ and different values of the transverse field parameter $(\rho_o/w_o) = 0.8$ (—), 1.2 ($\cdots\cdots$) and 2 ($- - -$).

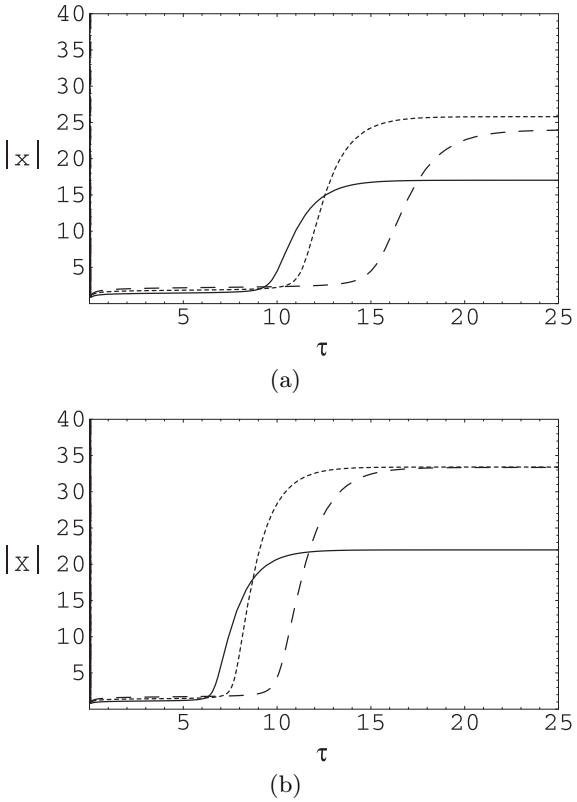

Fig. 14. (a) The transient output field $|X(\tau)|$ versus the time $\tau = \kappa t$ in the high-Q cavity limit in the NV case ($N = 0$) for $C = 20$, $\theta = 0$, $\delta = 0$, $\beta = 0.027$ and different $(\rho_o/w_o) = 0.8$ (—), 1.2 ($\cdots\cdots$) and 2 ($- - -$). (b) As (a) but in the SV case ($\Phi = \pi$, $N = 0.1$).

reduced for SV phase $\Phi = \pi$ (*or* $\pi/2$). For $\delta \neq 0$ and fixed (ρ_o/w_o) the time delay is reduced with $\delta = 0.5$ but increases again with $\delta = 1$ (Fig. 15). In either the NV or SV case the transition to the upper state is less steeper than the corresponding cases in the plane wave approximation.

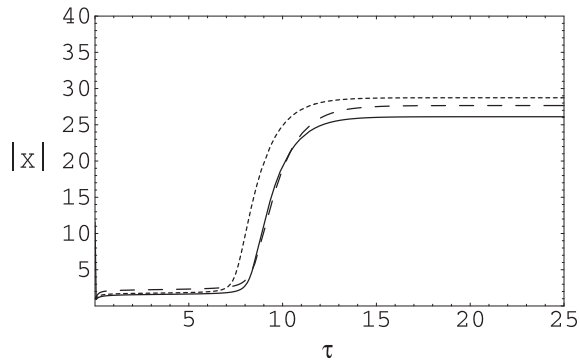

Fig. 15. As Figure 14a but in the SV case ($\Phi = \pi/2$, $N = 0.1$) for $C = 20$, $\theta = 0$, $\beta = 0.027$, $\rho_o/w_o = 1$ and different values of the atomic detuning $\delta = 0$ (—), 0.5 ($\cdots\cdots$) and $\delta = 1$ ($- - -$).

7 Summary

We have investigated the steady state behavior of the OB curves for an atomic model of 2-level structure placed in a ring cavity and in contact with squeezed vacuum (SV) field. Further to our previous study [5,6], in this work we have analysed the effect of the SV field parameters on the critical (switching-on) point within the plane wave approximation. The phenomenon of critical slowing down (CSD) related to the time switching response for the system to switch from the lower to the upper state of the OB curve is studied in detail in the following cases:

(i) in the high-Q cavity, the time delay near the switching-on point is reduced considerably for SV phase value $\Phi = \pi$ or further diverges for $\Phi = 0$ as compared with the NV case [14];
(ii) in the low-Q cavity, the switching time is both *enhanced* (due to reduction of fluctuation by SV field input) and *insensitive to the SV phase* (due to decorrelation of the SV photon twins by atomic collision). Otherwise, in the absence of collision broadening the transition to the upper state of the OB curve is accompained by the damped Rabi oscillations with shorter time-delay response in the SV case;
(iii) for arbitrary-Q cavity, the delay time reduces greatly with atomic detuning in the NV case, but it diverges with atomic detuning in the presence of the SV field;
(iv) the effect of the radial (transverse) Gaussian shape of the field in the high-Q cavity is to increase the time delay in the NV case, but it is reduced in the SV case with $\Phi = \pi$ and for (experimentally met [29]) transverse field parameter $(\rho_o/w_o) < 1$. Also the transition to the upper state of the OB curve with Gaussian transverse field feature is less steeper compared with the plane wave approximation in either the NV case [14] or the SV case as shown in the present work.

Finally, some comments are worth mentioning regarding our results within the semiclassical (SC) approximation which ignore the effects of quantum fluctuations:

(a) quantum analysis through a Fokker-Planck equation for OB systems in the NV case [30,31] shows that the

SC is valid for large cooperative parameter $C \gg 1$, i.e. by ignoring quantum fluctuation of $O\,(1/N_a)$ and smaller where N_a is the number of atoms;

(b) the SV input field has the effect of reducing the atomic quantum fluctuation and hence enhance the intrinsic stability of the system (represented by increased switching time delay in the low-Q cavity where dynamics is governed by atomic variables);

(c) as noted in [31] for the SC approximation to be valid "the applied driving field must be ramped in time intervals shorter than the characteristic time for random fluctuation" inherent in the system.

References

1. S.F. Hass, M. Sargent III, Opt. Comm. **79**, 366 (1990)
2. P. Galatola, L.A. Lugiato, M. Porreca, P. Tombesi, Opt. Comm. **81**, 175 (1991)
3. S.M.A. Maize, M.F.M. Ali, S.S. Hassan, Nonlin. Opt. **8**, 218 (1994)
4. J. Bergou, D. Zhao, Phys. Rev. A **52**, 1550 (1995)
5. S.S. Hassan, H.A. Batrafi, R. Saunders, R.K. Bullough, Eur. Phys. J. D **8**, 403 (2000); H.A. Batrafi, S.S. Hassan, R. Saunders, R.K. Bullough, Eur. Phys. J. D **8**, 417 (2000)
6. M.F.M. Ali, S.S. Hassan, S.M.A. Maize, J. Opt. B: Quant. Semiclass. Opt. **4**, 388 (2002)
7. R. Bonifacio, L.A. Lugiato, Opt. Comm. **19**, 172 (1976); Phys. Rev. A **18**, 1129 (1978); Lett. Nuovo Cim. **21**, 517 (1978); R. Bonifacio, M. Gronchi, L.A. Lugiato, Nuovo Cim. B **53**, 311 (1979)
8. S.L. McCall, Phys. Rev. A **9**, 1515 (1974); S.L. McCall, H.M. Gibbs, Opt. Comm. **33**, 335 (1980)
9. S.S. Hassan, P.D. Drummond, D.F. Walls, Opt. Comm. **27**, 480 (1978)
10. *Optical Bistability*, edited by C.M. Bowden, M. Ciftan, H.R. Robl (Plenum, NY, 1981); *Optical Bistability II*, edited by C.M. Bowden, H.M. Gibbs, S.L. McCall (Plenum, NY, 1984); *Optical Bistability III*, edited by H.M. Gibbs, P. Mandel, N. Peyghambarian, S.D. Smith (Springer, 1986); E. Abraham, D.D. Smith, Rep. Prog. Phys. **45**, 815 (1982)
11. L.A. Lugiato, L.M. Narducci, in *Fundamental Systems in Quantum Optics*, edited by J. Dalibard, J.M. Raimond, J. Zinn Justin (Elsevier Sci. Publ., Amsterdam, 1992), pp. 942-1043
12. P. Mandel, *Theoretical Problems in Cavity Nonlinear Optics* (Cambridge Univ. Press, Cambridge, 1997)
13. J.M. Yeomans, *Statistical mechanics of phase transitions* (Oxford Univ. press, Oxford, UK, 1997); L.E. Reichl, *A modern course in statistical physics* (Univ. of Texas press, USA, 1980)
14. R. Bonifacio, P. Meystre, Opt. Comm. **29**, 131 (1979)
15. T. Erneux, P. Mandel, Phys. Rev. A **28**, 896 (1983)
16. P. Mandel, T. Erneux, IEEE J. Quant. Electron. QE **21**, 1352 (1985)
17. S.S. Hassan, M.R. Wahiddin, R. Saunders, R.K. Bullough, Physica A **215**, 556; **219**, 482 (1995)
18. S.S. Hassan, H.A. Batrafi, R.K. Bullough, J. Opt. B: Quant. Semiclass. Opt. **2**, R35 (2000)
19. C.M. Savage, D.F. Walls, Phys. Rev. Lett. **57**, 2164 (1986)
20. R.J. Ballagh, J. Cooper, M.W. Hamilton, W.J. Sandle, W.M. Warrington, Opt. Comm. **37**, 143 (1981)
21. N.N. Rosanov, V.E. Semenov, Opt. Comm. **38**, 435 (1981)
22. E. Arimondo, A. Gozzini, L. Lovitch, E. Pistelli, in *Optical Bistability*, edited by C.M. Bowden, M. Ciftan, H.R. Robl (Plenum, NY, 1981), pp. 93-108
23. P.D. Drummond, IEEE J. Quant. Electron. QE **17**, 301 (1981)
24. J.V. Moloney, M.R. Belic, H.M. Gibbs, Opt. Comm. **41**, 379 (1982); J.V. Moloney, M. Sargent III, H.M. Gibbs, Opt. Comm. **44**, 289 (1983)
25. L.A. Lugiato, M. Milani, Z. Phys. B **50**, 171 (1983); L.A. Lugiato, R.J. Horowicz, G. Strini, L.M. Narducci, Phil. Trans. R. Soc. Lond. A **313**, 291 (1984)
26. W.J. Firth, I. Galbraith, E.M. Wright, J. Opt. Soc. Am. B **2**, 1005 (1985)
27. D. Weaire, J.P. Kermode, V.M. Dwjar, Opt. Comm. **55**, 223 (1985)
28. F. Xijun, T. Baoguo, Y. Zhifang, W. Xiang tai, Phys. Rev. A **44**, 2048 (1991)
29. F.T. Arecchi, G. Giusfredi, E. Petriella, P. Salieri, Appl. Phys. B **29**, 79 (1982)
30. P.D. Drummond, D.F. Walls, Phys. Rev. A **23**, 2563 (1981)
31. D.F. Walls, G.J. Milburn, *Quantum Optics* (Springer, 1995)